Food and Chemical Toxicology 126 (2019) 97–105

Contents lists available at ScienceDirect

Food and Chemical Toxicology

journal homepage: www.elsevier.com/locate/foodchemtox

Erianin protects against high glucose-induced oxidative injury in renal tubular epithelial cells

Mei-Fen Chen[a,b], Shorong-Shii Liou[c], Shung-Te Kao[a,d,**], I-Min Liu[c,*]

[a] School of Chinese Medicine, College of Chinese Medicine, China Medical University, Taichung, 40402, Taiwan
[b] College of Nursing, Chung Hwa University of Medical Technology, Rende Dist, Tainan City, 71703, Taiwan
[c] Department of Pharmacy and Master Program, Collage of Pharmacy and Health Care, Tajen University, Pingtung County, 90741, Taiwan
[d] Department of Chinese Medicine, China Medical University Hospital, Taichung, 40402, Taiwan

ARTICLE INFO

Keywords:
Erianin
Diabetic nephropathy
High glucose
NRK-52E cells
Mitogen-activated protein kinase
NF-κB

ABSTRACT

Erianin is the major bibenzyl compound found in *Dendrobium chrysotoxum* Lindl. The current study was designed to investigate the protective effects of erianin on high glucose-induced injury in cultured renal tubular epithelial cells (NRK-52E cells) and determine the possible mechanisms for its effects. NRK-52E cells were pretreated with erianin (5, 10, 25 or 50 nmol/L) for 1 h followed by further exposure to high glucose (30 mmol/L, HG) for 48 h. Erianin concentration dependently enhanced cell viability followed by HG treatment in NRK-52E cells. HG induced reactive oxygen species (ROS) generation, malondialdehyde production, and glutathione deficiency were recovered in NRK-52E cells pretreated with erianin. HG triggered cell apoptosis via the loss of mitochondrial membrane potential, depletion of adenosine triphosphate, upregulation of caspases 9 and 3, enhancement of cytochrome *c* release, and subsequent interruption of the Bax/Bcl-2 balance. These detrimental effects were ameliorated by erianin. HG also induced activation of p53, JNK, p38 mitogen-activated protein kinase (MAPK) and nuclear factor-κB (NF-κB) in NRK-52E cells, which were blocked by erianin. The results suggest that treatment NRK-52E cells with erianin halts HG-induced renal dysfunction through the suppression of the ROS/MAPK/NF-κB signaling pathways. Our findings provide novel therapeutic targets for diabetic nephropathy.

1. Introduction

Hyperglycemia and several other symptoms are involved in the development of complications associated with diabetes (Kreider et al., 2018). Diabetic nephropathy (DN) is not only considered a serious microvascular complication of diabetes, but also the principal cause of end-stage renal failure and cardiovascular mortality (Pugliese, 2014). Several mechanisms have been proposed to explain diabetic renal disease by hyperglycemia. In the state of hyperglycemic, overproduction of reactive oxygen species (ROS) and free radicals overwhelms the intrinsic antioxidant system and reduced glutathione (GSH) levels resulting in oxidative stress (Rani et al., 2016; Volpe et al., 2018). The overproduction of intracellular oxidative stress in response to hyperglycemia can occur in mitochondria that trigger DNA damage and ultimately leads to the apoptosis of renal cells (Yang et al., 2017; Sifuentes-Franco et al., 2018). There is considerable evidence that the induction of apoptosis involves several critical steps: disturbance of Bcl-2 family protein balance, reduction of mitochondrial transmembrane potential with concomitant release of mitochondrial protein cytochrome *c* and the subsequent activation of caspases (Luna-Vargas and Chipuk, 2016; Vakifahmetoglu-Norberg et al., 2017). Mitogen activated protein kinases (MAPKs) and nuclear factor-κB (NF-κB) signaling pathways also play a crucial role in tissue inflammation and cell apoptosis, and it is activated by hyperglycemia (Sakai et al., 2005; Sanchez and Sharma, 2009). Therefore, regulation on oxidative stress, mitochondrial dysfunction and associated cell death would be an important approach to protect renal cells against high glucose induced injury (Yang et al., 2017; Sifuentes-Franco et al., 2018).

Traditional Chinese medicine (TCM) considers that the debilitating kidney and the stagnation of the kidney collateral are critical to the pathogenesis of DN (Lv et al., 2018). According to the theory of TCM, strengthening the spleen and tonifying the kidney kidney as well as removing blood stasis and dredging collaterals could play an important role in the treatment of DN (Lv et al., 2018). *Dendrobium* species

* Corresponding author. Department of Pharmacy and Master Program, Collage of Pharmacy and Health Care, Tajen University, 90741, Pingtung County, Taiwan.
** Corresponding author. School of Chinese Medicine, College of Chinese Medicine, China Medical University, 40402, Taichung, Taiwan.
E-mail addresses: stkao@mail.cmu.edu.tw (S.-T. Kao), iml@tajen.edu.tw (I.-M. Liu).

https://doi.org/10.1016/j.fct.2019.02.021
Received 14 December 2018; Received in revised form 17 January 2019; Accepted 8 February 2019
Available online 11 February 2019
0278-6915/

(Orchidaceae) are the tonic herbs in Chinese medicine has been used for the promoting the secretion of body fluid, benefiting the stomach, moistening lung and tonifying kidney and improving eyesight (Lam et al., 2015). Thus, chemical components and pharmacology of *Dendrobium* plants have been studied to provide scientific proof to justify the medicinal use in treatment of diseases (Lam et al., 2015). *Dendrobium chrysotoxum* Lindl., a species of medicinal *Dendrobium* (Shihu in Chinese) indexed in the Chinese Pharmacopoeia (2010 version), is often used as antipyretic and analgesic medication in TCM (Chinese Pharmacopeia Commission, 2010). In addition, the *in vivo* studies have been shown that *D. chrysotoxum* attenuated the development of diabetic retinopathy (DR) by inhibiting retinal angiogenesis and inflammation (Gong et al., 2014; Yu et al., 2015). Erianin [2-Methoxy-5-(2-(3,4,5-trimethoxyphenyl)-ethyl)-phenol] is the major bibenzyl present in *D. chrysotoxum*, and this compound is generally used as the chemical marker for the quality control of *D. chrysotoxum* (Hu et al., 2012). Previous studies have demonstrated that erianin can elicit multiple pharmacological effects, including anti-oxidative and antitumor activities (Ma et al., 1994; Ng et al., 2000). Actually, erianin is able to ameliorates DR by blocking high glucose-induced retinal angiogenesis (Yu et al., 2016). Erianin seems to possess a multitude of biological activities to improve factors associated with diabetic microvascular complications, and this coumpoud could be a suitable drug candidate for the treatment and prevention of DN. However, there is no comprehensible evidence relating to the protective role of erianin on DN.

It is known that renal proximal tubule cells are more prone to hyperglycaemia-induced cellular apoptosis and injury, therefore, renal proximal tubule cells lesions play a pivotal role in the development of DN (Vallon and Thomson, 2012; Czajka and Malik, 2016). The normal rat renal (NRK-52E) cells maintain the characteristics of normal renal proximal tubular cells, and have been used extensively in the study of proximal tubule cell functions (Slyne et al., 2015). When NRK-52E cells were cultured in high glucose (HG) medium, the elevated ROS state caused the cells to going into apoptosis (Zhang et al., 2014). Therefore, the NRK-52E cells could be recognized as an *in vitro* model system for examining the mechanisms that underlie HG-mediated injury and the subsequent development of experimental and clinical DN (Slyne et al., 2015). The current study was designed to investigate the protective effects of erianin on HG-induced injury in NRK-52E cells as an *in vitro* cellular model for DN and determine the possible mechanisms for its effects.

2. Materials and methods

2.1. Cell culture

A normal rat kidney epithelial cell line (NRK-52E) were purchased from Bioresource Collection and Research Center (BCRC 60086) of the Food Industry Research and Development Institute (Hsinchu, Taiwan). The cells were cultured in Dulbecco's Modified Eagle Medium (DMEM) supplemented with 10% foetal bovine serum (FBS), 1% L-glutamine, and 1% penicillin/streptomycin, at 37 °C in a 5% CO_2 incubator for 24 h, and were replaced to new medium every 2–3 days. For all experiments, cells were cultured in serum-free conditions for 24 h when they reached 80% confluence.

2.2. High-glucose stimulation and treatments

Cells were seeded at a density of 2×10^6 cells/well in 6-well plates. Upon confluence, cultures were passaged by dissociation in 0.05% (w/v) trypsin (Sigma-Aldrich, St. Louis, MO, USA) in phosphate-buffered saline (PBS) pH 7.4. Cells were maintained in fresh medium containing 1% FBS for 2 h prior to use in the experiments. Later, cells were pretreated with erianin (Chengdu Must Bio-Technology Co. Ltd., Chengdu, China, purity ≥98%) at different concentrations (5, 10, 25 or 50 nmol/L), or vehicle (dimethyl sulfoxide; DMSO, Sigma-Aldrich) for 1 h followed by exposure to normal glucose (NG, 5.5 mmol/L glucose) or high glucose (HG, 30 mmol/L glucose) for 48 h without medium change. The dosage regimen was selected based on a previous report demonstrating that these concentrations of erianin were able to inhibit HG-induced tube formation and migration in the monkey choroidal retinal vascular endothelial cell line without cytotoxicity (Yu et al., 2016). Erianin powder was dissolved in DMSO to create a 100 μmol/L stock solution, which was subsequently diluted in culture medium to the appropriate concentrations for subsequent experiments. The final DMSO concentration was less than 0.1% (v/v), a concentration that did not affect cell viability. The final DMSO concentration did not exceed 0.1% (v/v), a concentration that did not affect cell viability. Afterwards, cell viability, antioxidant enzyme activities, reactive oxygen species (ROS) generation, and several apoptotic indexes were assessed. Triple wells were evaluated in each experiment, and each experiment was performed at least five times independently.

2.3. Cell viability assay

The viability of NRK-52E cells was determined by a c3-(4, 5-dimethylthiazol-2-yl)-2,5 diphenyl tetrazolium bromide (MTT) and lactate dehydrogenase (LDH) assay (Gerlier and Thomasset, 1986; Rastogi et al., 2010). Briefly, cells were seeded in 96-well plates at a density of 8×10^3 cells per well and incubated for 24 h. Subsequently, cells were pretreated with erianin at different concentrations for 1 h and then exposed to NG or HG medium for an additional 48 h. At the end of the incubation period, the supernatant was drew from the media of per well and centrifuged at $400 \times g$ for 5 min at 4 °C, then 20 μL supernatant was transferred into another 96-well microplate to determine LDH levels prior to adding MTT. Release of LDH into the media was measured by using a commercial assay kit (Abcam plc., Cambridge, MA, USA, Cat. No. ab101526). For the MTT assay, the cells in each well were washed with PBS and 100 μL (0.5 mg/mL) of MTT (Sigma-Aldrich) solution was added to each well. After a 4 h incubation at 37 °C, the MTT solution was discarded and 100 μL of DMSO was added to each well and shaken for 5 min to solubilize the formazan formed in the viable cells. The optical density (OD) was measured using a microplate reader (SpectraMax M5, Molecular Devices, USA) at 450 nm. Each experiment was performed in three wells and was triplicated at least five times.

2.4. Detection of intracellular ROS

The generation of intracellular ROS was assessed using 2,7-dichlorofluorescein diacetate (DCFDA), a non-fluorescent probe, which is converted to the highly fluorescent derivative dichlorofluorescin due to oxidation by ROS and peroxides (Kaja et al., 2017). We used a DCFDA Cellular ROS Detection Assay Kit (Abcam plc., Cat. No. ab113851), following the manufacturer's instructions. In brief, an aliquot of the isolated cells (8×10^6 cells/mL) was made up to a final volume of 2 mL in normal phosphate-buffered saline (PBS; pH 7.4). Then, a 1-mL aliquot of cells was added to 100 μL of DCFDA (10 μmol/L) and incubated at 37 °C for 30 min and washed twice with PBS. Cells were solubilized in Triton-X100 1% (vol/vol) in distilled water. The cells were then examined under a fluorescence microscope (Nikon). The percentage of fluorescence-positive cells was measured at an excitation wavelength of 488 nm and an emission wavelength of 525 nm using a multi-detection microplate reader (SpectraMax M5).

2.5. Measurement of lipid peroxidation

Lipid peroxidation was studied by measuring the amount of malondialdehyde (MDA) in the cell homogenates using the lipid peroxidation assay kit (Abcam plc., Cat. No. ab118970) as per the manufacturer's instructions. Briefly, 1 mmol/L ethylene diamine tetraacetic acid (Sigma-Aldrich) was added to a 0.5 mL cell lysate (6×10^6 cells/mL) and was mixed with 1 mL cold 15% (w/v) thiobarbituric acid

(TBA) to precipitate proteins. The supernatant was treated with 1 mL 0.5% (w/v) TBA in a boiling water bath for 15 min. After cooling, the absorbance was read at 535 nm and the concentration of the thiobarbituric acid reactive substance in the sample solution was expressed as nmol/ml using a standard solution containing a known concentration of MDA (Esterbauer and Cheeseman, 1990). Total protein concentrations were measured according to the method described in Lowry et al. (1951).

2.6. Measurement of glutathione/oxidized glutathione ratio

The ratio of glutathione (GSH) to glutathione disulfide (GSSG) was used to determine the cellular redox status. The ratio was measured with a kit from Cayman (Ann Arbor, MI, USA), which used a spectrophotometric recycling assay to measure cellular levels of GSH and GSSG. Briefly, following treatments, cells were scrape-harvested in cold PBS on ice and centrifuged. The cell pellets were frozen at −80 °C. Cells were thawed and homogenized in cold 2-(N-morpholino)ethanesulfonic acid (MES) buffer (0.2 mol/L MES, 50 mmol/L phosphate, 1 mmol/L EDTA, pH 6.0) and centrifuged at 10,000 *g* for 15 min at 4 °C. The supernatants were removed for the assay according to the manufacturer's instruction. All the results were normalized to total cellular protein content. The absorbance was recorded at 405 nm using a plate reader at 5 min intervals for 30 min.

2.7. Measurement of mitochondrial membrane potential

A mitochondrial membrane potential assay kit containing JC-1 (Abcam plc., Cat. No. ab113850) was used to measure the mitochondrial membrane potential in cells. Briefly, 1×10^4 cells were laid in a 96-well plate and incubated with 20 μmol/L JC-1 in growth medium at 37 °C for 30 min. Monomeric JC-1 green fluorescence emission (530 nm) and aggregate JC-1 red fluorescence emission (590 nm) were determined using a fluorescence spectrophotometer (F-2500; Hitachi). The mitochondrial membrane potential in each group was calculated as the fluorescence ratio of red to green. This value was adjusted by subtracting the value obtained from the carbonyl cyanide 3-chlorophenylhydrazone incubation and expressed as a percentage of the vehicle control.

2.8. Measurement of adenosine triphosphate (ATP) levels

ATP levels were measured using a bioluminescence assay based on the ability of luciferase to produce light in the presence of its substrate luciferin and ATP (Kimmich et al., 1975). In brief, after treatment, the cells were lysed with 10% tricholoroacetic acid, neutralized with 1 mol/L KOH and diluted with 100 mmol/L HEPES buffer (pH 7.4). Then, 50 μL neutralized extract was injected into a cuvette containing 10 μL luciferin (Sigma-Aldrich), 10 μL $MgSO_4$ and 10 μL luciferase. Luminescence was recorded with a SpectraMax M5 multimode microplate. The luminescence then was normalized to total protein concentration.

2.9. Quantification of apoptosis

The cell death detection ELISA kit (Roche Molecular Biochemicals, Mannheim, Germany, Cat. No.11544675001) was used to quantitatively detect the cytoplasmic histone-associated DNA fragments after induced cell death. Briefly, the cells were seeded at a density of 2.4×10^5 cells/well in 6-well plates. After treatment, cytoplasmic extracts from cells were used as an antigen source in a sandwich ELISA with a primary anti-histone mouse monoclonal antibody coated to the microtiter plate and a second anti-DNA mouse monoclonal antibody coupled to peroxidase. The amount of peroxidase retained in the immunocomplex was determined photometrically by incubating with 2,2′-azino-di-[3-ethylbenzthiazoline sulfonate] (ABTS) as a substrate for 10 min at 20 °C. The change in color was measured at a wavelength of 405 nm by using a Dynex MRX plate reader controlled through PC software (Revelation, Dynatech Laboratories, CA). The optical density reading was then normalized to the total amount of protein in the sample and the data were reported as an apoptotic index (OD_{405}/mg protein) to indicate the level of cell death.

2.10. Western blot analysis

The mitochondrial fractionation kit (Active Motif, Inc., Carlsbad, CA, USA, Cat. No. 40015) was used to isolate cytosolic and mitochondrial fractions from cells according to the manufacturer's instructions. For the extraction of nuclear and cytoplasmic proteins of cells, a Nuclear Extract Kit (Active Motif, Inc., Cat. No. 40010) was used according to the protocol. Protein concentrations were determined using the Bradford protein assay (Bio-Rad Laboratories). Equal amounts of protein (50 μg/lane) were resolved by electrophoresis for Western blot analysis. Protein was separated by electrophoresis on 10% sodium dodecyl sulfate-polyacrylamide gel electrophoresis and transferred electrophoretically to polyvinylidene difluoride membranes. Membranes were blocked with 5% non-fat dry milk in Tris-buffered saline Tween (20 mmol/L Tris, pH 7.6, 137 mmol/L NaCl, and 0.1% Tween 20) for 3 h at room temperature, accompanied by an overnight incubation at 4 °C with primary antibodies against cytochrome c (Santa Cruz Biotechnology, Inc., Santa Cruz, CA, USA, Cat. No.13156), cleaved caspase-3 (Cell Signaling Technology, Beverly, CA, USA, Cat. No. 9661), cleaved caspase-9 (Cell Signaling Technology, Cat. No. 9501), p53 (Cell Signaling Technology, Cat. No.9282), p-p53 (Ser15) (Cell Signaling Technology, Cat. No. 9284), Bcl-2 (Santa Cruz Biotechnology, Inc., Cat. No. sc-492), Bax (Santa Cruz Biotechnology, Inc., Cat. No. sc-526), NF-κB p65 (Santa Cruz Biotechnology, Inc.; Cat. No. sc-109), JNK (Santa Cruz Biotechnology, Inc., Cat. No. sc-137020), p-JNK (Thr 183/Tyr 185) (Santa Cruz Biotechnology, Inc., Cat. No. sc-6254), p38 (Cell Signaling Technology, Cat. No. 9212), or p-p38 (Thr180/Tyr182) (Cell Signaling Technology, Cat. No. 9211). The β-actin antibody (Santa Cruz Biotechnology, Inc., Cat. No. sc-130656) was used as an internal control in immunoblotting. The cytochrome c oxidase subunit IV isoform 1 (Cox IV) antibody (Cell Signaling Technology, Cat. No. 4850) was used as a mitochondrial loading control. The lamin B1 antibody (Santa Cruz Biotechnology, Inc., Cat. No. sc-56143) was used as a nuclear loading control. All antibodies were used at a dilution of 1:1000. After being washed three times with Tris-buffered saline Tween 20 (TBST), incubation with the appropriate horseradish peroxidase-conjugated secondary antibodies was performed for one hour at room temperature. After three additional TBST washes, the immunoreactive bands were visualized by enhanced chemiluminescence (Amersham Biosciences, Buckinghamshire, UK) as per the manufacturer's instructions. Band densities were calculated with ATTO Densitograph Software (ATTO Corporation, Tokyo, Japan) and quantified as the ratio to β-actin, COX IV or lamin B1. The mean value for samples from the vehicle treated cells cultured under normal glucose on each immunoblot, expressed in densitometry units, was adjusted to a value of 1.0. All experimental sample values were then expressed relative to this adjusted mean value. All determinations were performed in triplicate, and each experiment was repeated at least five times.

2.11. NF-kB DNA-binding assay

In order to determine the role of JNK and p38 in activation of NF-κB in renal tubular epithelial cell apoptosis under HG condition, the NRK-52E cells were pretreated with the p38 inhibitor (SB203580; Sigma-Aldrich), or JNK inhibitor (SP600125; Sigma-Aldrich) at 10 μmol/L for 30 min and then incubated with erianin (50 nmol/L) or vehicle for 1 h followed by exposure to NG or HG medium for 48 h. Nuclear extract of cells was prepared using the nuclear extract kit (Active Motif, Inc., Cat. No. 40410) following manufacturer's protocol. DNA-binding activity of NF-kB was quantified using the TransAM® NF-κB p65 transcription

factor assay kit (Active Motif, Inc., Cat. No. 40596), according to the manufacturer's protocol. Optical density was measured at 450 nm as a relative measure of protein bound NF-kB.

2.12. Statistical analysis

Data are expressed as the mean ± standard deviation (SD). Statistical analysis and graphics were performed with a SigmaPlot 12.3 program (version 2016, Systat Software Inc., San Jose, CA, USA). Statistical analysis was performed with one-way analysis of variance (ANOVA). Dunnett range post-hoc comparisons were used to determine the source of significant differences, where appropriate. A p-value < 0.05 was considered statistically significant.

3. Results

3.1. Effect of erianin on HG-Induced cytotoxicity in NRK-52E cells

In an MTT test, cell viability was approximately 58.4% in HG-cultured cells, whereas erianin prevented cell death caused by HG in a concentration-dependent manner, with almost 92.1% of the cells surviving at 50 nmol/L of erianin (Fig. 1A).

In a cell viability test based LDH release rate, treatment of NRK-52E cell with HG for 48 h induced cytotoxicity as the LDH release rate was increased to 183.6% of the control value in the NG medium (Fig. 1B). When the HG-cultured cells were treated with different concentrations (5, 10, 25 or 50 nmol/L) of erianin, the LDH release rate was significantly decreased (166.2, 145.9, 129.5 and 113.2% of the control value in the NG medium, respectively) in a concentration-dependent manner.

3.2. Effects of erianin on ROS production, lipid peroxidation and the ratio of oxidized/reduced glutathione in NRK-52E cells cultured in HG medium

The intracellular levels of ROS and MDA in NRK-52E cells were higher by about 2.2-, and 4.7-fold, respectively, in HG-cultured cells when compared to the vehicle-treated group cultured in NG medium (Fig. 2A and B). The higher levels of ROS and MDA in NRK-52E cells under HG medium were reduced by erianin (50 nmol/L) treatment with a decrease of 47.9 and 58.4%, respectively, relative to those observed in the vehicle-treated counterparts (Fig. 2A and B).

As shown in Fig. 2C, the GSH/GSSG ratio significantly declined in NRK-52E cells exposed to HG medium, but pretreatment with erianin significantly increased this ratio in a concentration dependent manner.

3.3. Effects of erianin on HG-induced mitochondrial dysfunction in NRK-52E cells

The mitochondrial membrane potential in erianin cells exposed to HG medium was reduced to 52.1% of that in the NG group (Fig. 3A). Treatment of HG-cultured NRK-52E cells with erianin increased mitochondrial membrane potential in a concentration-dependent manner (Fig. 3A).

NRK-52E cells exposed to HG medium displayed a significant decline in ATP level (Fig. 3B). Pre-treatment of NRK-52E cells with erianin significantly increased HG reduced ATP level in a concentration-dependent manner (Fig. 3B).

It was shown that decreased mitochondrial levels of cytochrome c were followed by increased cytosolic levels in NRK-52E cells cultured under HG medium, while erianin inhibited the release of cytochrome c from mitochondria to cytoplasm in a concentration-dependent manner (Fig. 3C).

HG caused a 3.8-fold increase in the rate of apoptosis in NRK-52E cells and erianin treatment attenuated this increase in a concentration dependent manner (Fig. 3D). The rate of apoptosis decreased by 54.2% in HG cultured NRK-52E cells pretreated with 50 nmol/L erianin relative to the vehicle-treated counterpart group (Fig. 3D).

3.4. Effects of erianin on the apoptotic and anti-apoptotic factors in NRK-52E cells cultured in HG medium

HG caused a 4.2-fold and 4.0-fold increase in cleaved caspase-9 and cleaved caspase-3 protein expression in NRK-52E cells (Fig. 4A). The protein expression of cleaved caspase-9 and cleaved caspase-3 in HG-cultured NRK-52E cells was sharply decreased (70.9 and 52.3% reduction, respectively) by treatment with erianin (50 nmol/L) when compared to those of the vehicle-treated counterparts (Fig. 4A).

The immunoblot results showed that the level and phosphorylation degree of p53 were 3.2- and 4.5-fold greater, respectively, in the HG cultured NRK-52E than in vehicle-treated group cultured in NG medium (Fig. 4B). Treatment of HG cultured NRK-52E cells with erianin (50 nmol/L) downregulated the level and phosphorylation degree of p53 to 1.5- and 1.6-fold of those in the vehicle-treated group cultured in NG medium (Fig. 4B). HG caused a 1.4-fold increase in the p-p53/p53 ratio in NRK-52E cells (Fig. 4B). The ratio of p-p53/p53 was decreased to 54.2% in HG cultured NRK-52E cells pretreated with 50 nmol/L erianin when compared to those of the vehicle-treated counterparts (Fig. 4B).

HG greatly increased the Bax/Bcl-2 ratio in NRK-52E cells (by 17.1-fold relative to that seen in the vehicle-treated group cultured in NG medium; Fig. 4C). This HG-induced up-regulation in the Bax/Bcl-2 ratio was reversed in NRK-52E cells after treatment with 50 nmol/L erianin, with a 81.2% decrease when compared to that of their vehicle-treated counterpart group (Fig. 4C).

3.5. Effects of erianin on the activation of MAPK and NF-κB in NRK-52E cells cultured in HG medium

The immunoblot results showed that the ratio of p-pJNK/pJNK and p-p38/p38 were 4.3- and 4.5-fold greater, respectively, in the HG

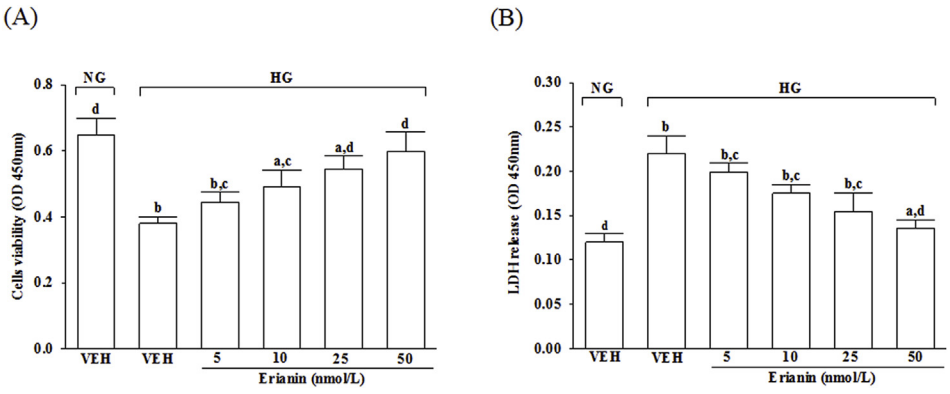

Fig. 1. Effect of erianin on cell viability in NRK-52E cells following high glucose exposure. Cells were pretreated with different concentrations of erianin (5, 10, 25 or 50 nmol/L) for 1 h and then exposed to normal (NG) or high (HG) glucose for an additional 48 h. Cell viability was measured by (A) MTT assay and (B) LDH release assay. The experiments were performed in triplicate and data are presented as mean ± S.D. of five independent experiments (n = 5). $^{a}p < 0.05$ and $^{b}p < 0.01$ when compared to the vehicle (VEH)-treated control group cultured in NG medium. $^{c}p < 0.05$ and $^{d}p < 0.01$ when compared to the VEH-treated group cultured in HG medium.

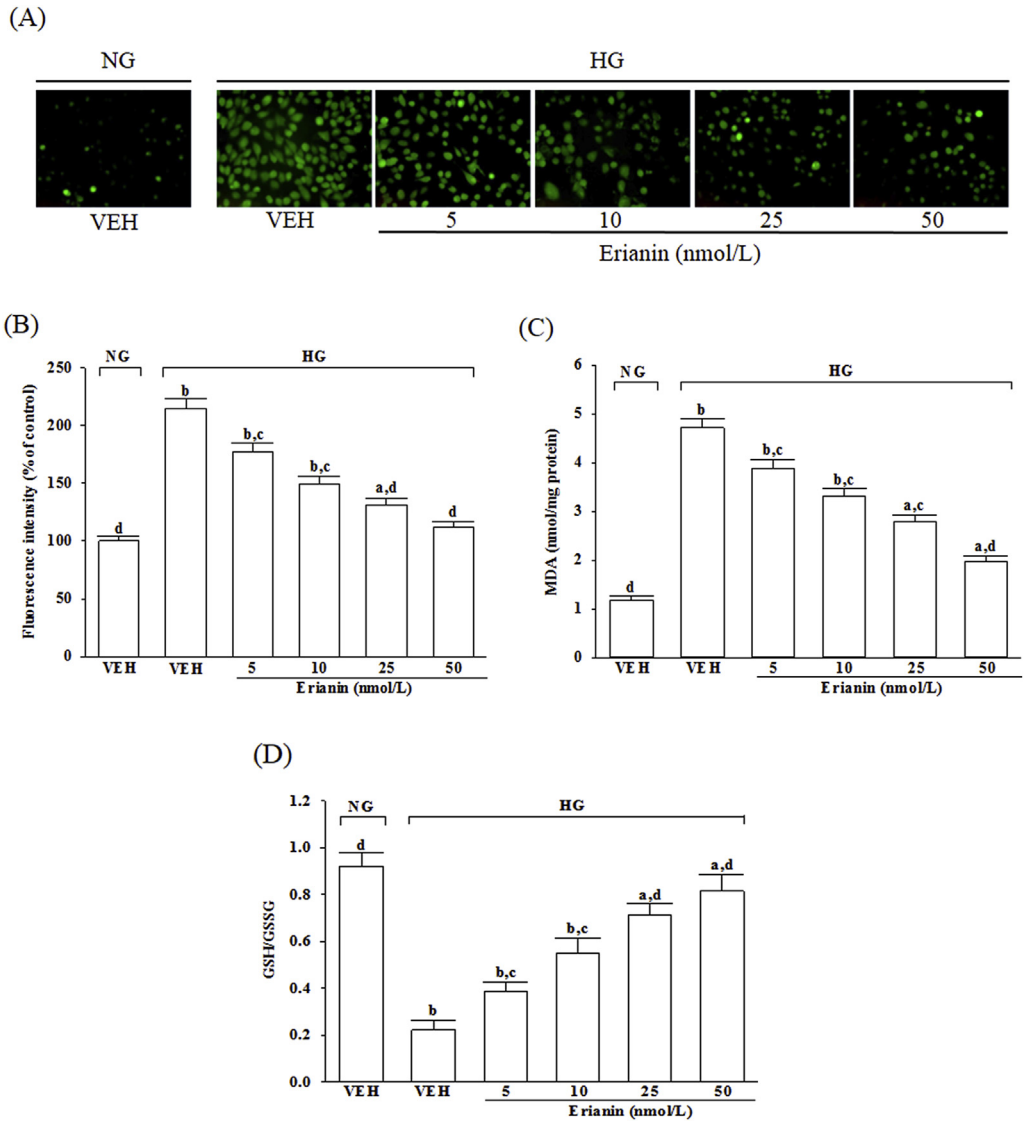

Fig. 2. Effects of erianin on ROS production, lipid peroxidation, and GSH/GSSG ratio in NRK-52E cells cells following high-glucose challenge. Cells were pretreated with different concentrations of erianin (5, 10, 25 or 50 nmol/L) for 1 h and then exposed to normal (NG) or high (HG) glucose for an additional 48 h. (A) Changes in ROS production were determined by image analysis of DCFDA-loaded cells on a fluorescent microscope. Magnification: x100. (B) Fluorescence was measured with a multifunctional microplate reader at an excitation wavelength of 488 nm and an emission wavelength of 525 nm for ROS. (C) Lipid peroxidation was estimated by measuring the level of MDA production using the thiobarbituric acid method. (D) The GSH/GSSG ratio in the cells was measured using a commercial kit. The experiments were performed in triplicate and data are presented as mean ± S.D. of five independent experiments (n = 5). $^{a}p < 0.05$ and $^{b}p < 0.01$ when compared to the vehicle (VEH)-treated control group cultured in NG medium. $^{c}p < 0.05$ and $^{d}p < 0.01$ when compared to the VEH-treated group cultured in HG medium.

cultured NRK-52E than in vehicle-treated group cultured in NG medium (Fig. 5A). Compared to those in the vehicle-treated group cultured in NG medium, treatment of HG cultured NRK-52E cells with erianin (50 nmol/L)) downregulated the ratio of p-pJNK/pJNK and p-p38/p38 to 1.7- and 1.2-fold (Fig. 5A). The levels of total p38 and JNK protein did not change in NRK-52E cells treated with high glucose in the presence or absence of erianin (Fig. 5A).

The nuclear-to-cytosolic protein expression ratio of NF-κB p65 protein was 13.2-fold higher in the HG cultured NRK-52E cells compared to that in the NG vehicle-treated group (Fig. 5B). Erianin (50 nmol/L) suppressed the nuclear-to-cytosolic protein expression ratio of NF-κB p65 protein in the high glucose cultured NRK-52E cells by 16.1% relative to that seen in their vehicle-treated counterpart group (Fig. 5B).

The DNA-binding activity of NF-kB p65 was 2.4-fold higher in the HG cultured NRK-52E cells than in the NG vehicle-treated group, which were lowered by 50 nmol/L erianin treatment, with a reduction of 26.2%, when compared with the levels observed in the vehicle-treated counterparts (Fig. 5C). SB203580 or SP600125 significantly inhibited the HG-induced DNA-binding activity of NF-kB p65, but did not affect the inhibitory effect of erianin in the HG cultured NRK-52E cells (Fig. 5C).

4. Discussion

The main characteristic in all forms of diabetes is hyperglycaemia, which induced oxidative stress and disrupted the balance between ROS generation and the innate cell's ability to scavenge the reactive species, thus play a primary role in the pathogenesis of micro- and macrovascular diabetic complications (Volpe et al., 2018). Accumulating evidence indicates that renal tubular injury plays a critical role in the pathogenesis of human and animal DN (Vallon and Thomson, 2012; Czajka and Malik, 2016). Thus, rat NRK-52E renal tubular epithelial cells cultured under HG conditions were employed as a model of DN (Slyne et al., 2015). Erianin is a phenolic substance extracted from plants in *D. chrysotoxum* (Chinese Pharmacopeia Commission, 2010). As *D. chrysotoxum* has been report to posess the ability to attenuat the development of diabetic microvascular injury (Gong et al., 2014; Yu et al., 2015), the current study used the *in vitro* approach to examine whether erianin is also the active compound of *D. chrysotoxum* on the HG-induced NRK-52E cells.

When the ROS level exceeds the capacity of the antioxidant defense system, ROS initiates chain reactions by oxidizing cellular macromolecules like lipids and proteins, which in turn interrupts cellular activities, ultimately causing apoptosis (Volpe et al., 2018). The increase in MDA level is associated with the oxidative damage of membrane lipids since ROS in cells exposed to a HG environment are

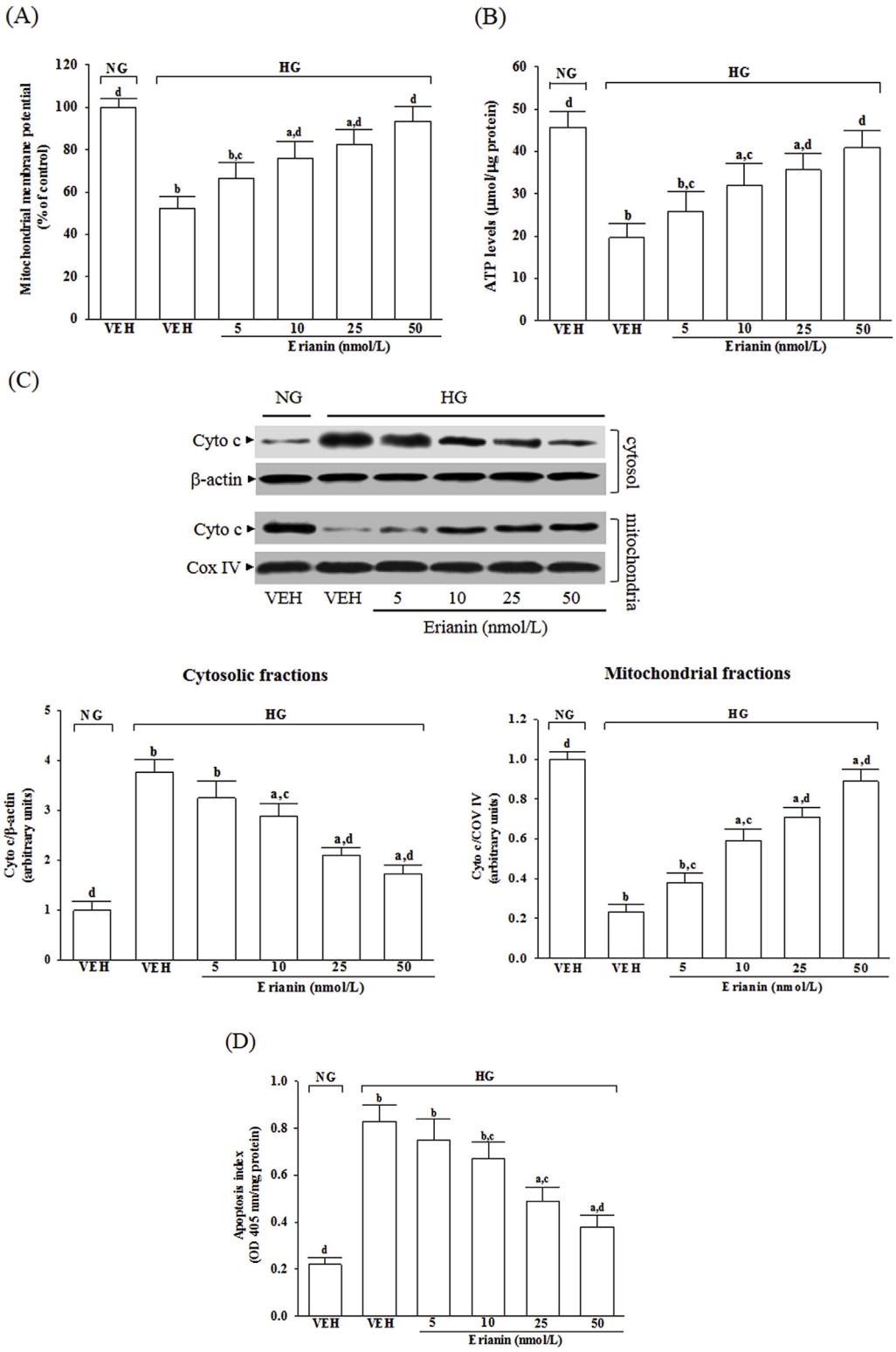

Fig. 3. Effects of erianin on high glucose-induced mitochondrial dysfunction in NRK-52E cells. Cells were pretreated with different concentrations of erianin (5, 10, 25 or 50 nmol/L) for 1 h and then exposed to normal (NG) or high (HG) glucose for an additional 48 h. (A) Mitochondrial membrane potential was assessed using JC-1 dye. (B) ATP production was measured by luciferin-luciferase assay. (C) The photographs were representatives the Western blots for the expression of cytochrome c (Cyto c) in the cytosolic and mitochondrial fractions. The relative expression levels of cytochrome c in the cytosolic and mitochondrial fractions of cells are listed in the lower pannels. (D) The apoptosis index was measured by detection of DNA fragmentation with the cell death detection ELISA kit. The experiments were performed in triplicate and data are presented as the mean ± S.D. of five independent experiments (n = 5). $^{a}p < 0.05$ and $^{b}p < 0.01$ when compared to the vehicle (VEH)-treated control group cultured in NG medium. $^{c}p < 0.05$ and $^{d}p < 0.01$ when compared to the VEH-treated group cultured in HG medium.

elevated (Tsikas, 2017). In accordance with previous studies described, higher MDA in NRK-52E cells cultured under HG medium were observed (Zhao et al., 2015). From this observation, an increase in HG-induced oxidative damage of the cell membrane was suggested. By cycling between two forms of GSH and GSSG, glutathione serves as an electron donor to unstable ROS, and thus, the ratio of oxidized/reduced glutathione has been noted as an index of oxidative stress (Németh and Boda, 1989; Owen and Butterfield, 2010). The present study showed that GSH/GSSG ratio was significantly diminished in NRK-52E cells under high glucose stress, which supports previous studies suggesting that cell susceptibility to oxidative stress is closely related to the extent of GSH/GSSG redox imbalance (Németh and Boda, 1989; Owen and Butterfield, 2010). Pretreatment of NRK-52E cells with erianin inhibited the HG-induced ROS generation and lipid peroxidation and also abrogated the reduction of the GSH/GSSG ratio. Given that oxidative stress mechanisms lead to DN, a logical therapeutic approach is to prevent oxidative stress by increasing antioxidant defense (Sifuentes-Franco et al., 2018). These data revealed that the protective effects of

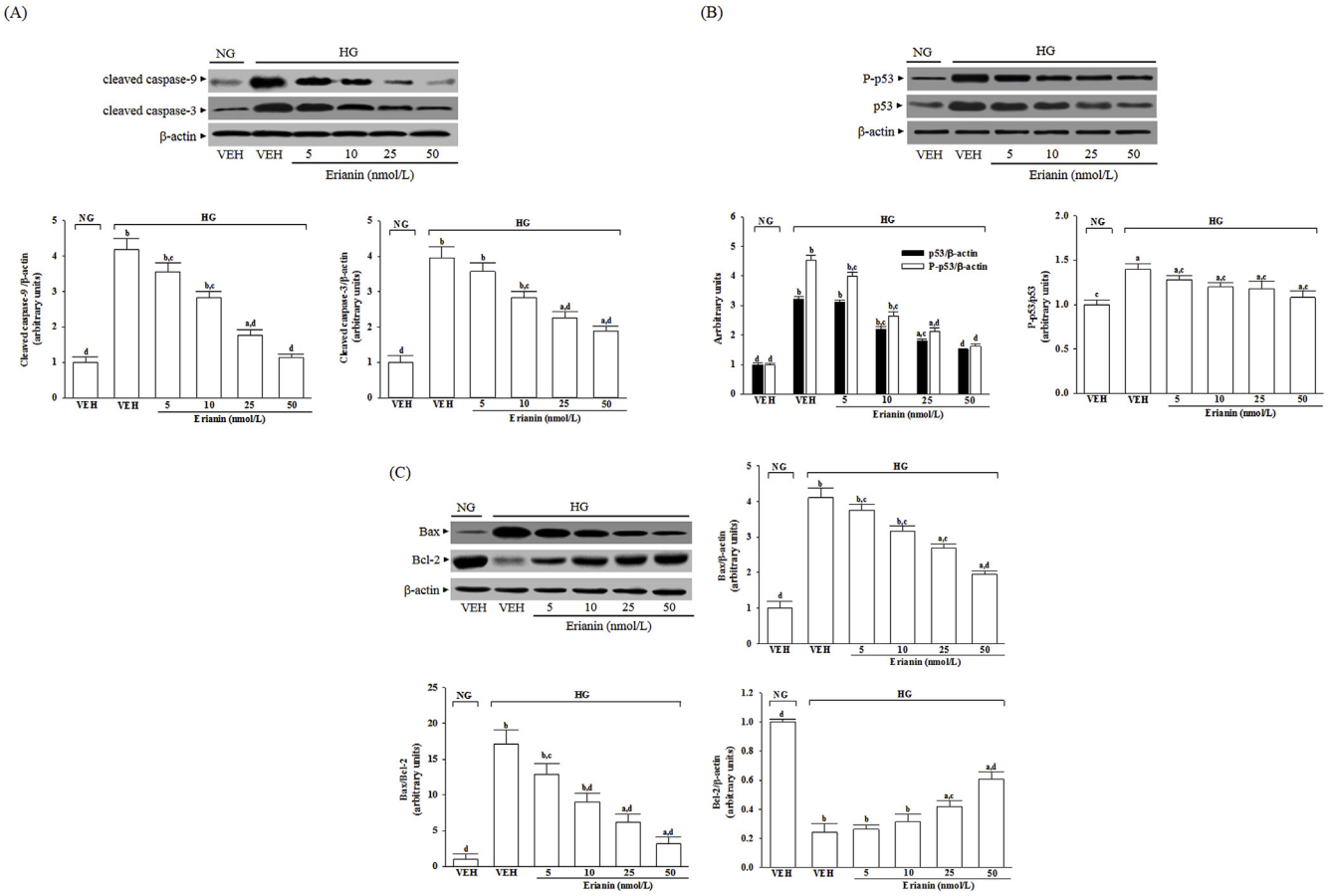

Fig. 4. Effects of erianin on protein expression related to apoptosis in NRK-52E cells under high glucose conditions. Cells were pretreated with different concentrations of erianin (5, 10, 25 or 50 nmol/L) for 1 h and then exposed to normal (NG) or high (HG) glucose for an additional 48 h. The photographs are representative the Western blots for (A) cleaved caspase-9 and cleaved caspase-3, (B) p-p53 and p53, (C) Bax and Bcl-2. The densities of protein bands were quantitated and listed in the lower pannels. The experiments were performed in triplicate and data are presented as the mean ± S.D. of five independent experiments (n = 5). $^{a}p < 0.05$ and $^{b}p < 0.01$ when compared to the vehicle (VEH)-treated control group cultured in NG medium. $^{c}p < 0.05$ and $^{d}p < 0.01$ when compared to the VEH-treated group cultured in HG medium.

erianin on HG induced oxidative stress injury in NRK-52E cells might be contribute to balance the oxidative stress and antioxidant systems.

Mitochondria is the primary intracellular site of oxygen consumption and the major source of ROS (Sinha et al., 2013). The upregulated production of intracellular ROS induced by HG can damage mitochondrial membrane lipids and lead to a reduction in mitochondrial membrane potential, which is associated with an absolute decrease in ATP and ultimately, disrupts the electron transfer chain and causes cell death (Pérez and Quintanilla, 2017). The loss of mitochondrial membrane potential increases mitochondrial permeability leading to mitochondrial swelling, rupture of the outer mitochondrial membrane, followed by release of cytochrome c from mitochondria into cytosol, which triggers apoptotic cell death through caspase activation (Hüttemann et al., 2012). Mitochondrial dysfunction seems to be a central mediator of neural apoptosis in DN (Sifuentes-Franco et al., 2018). We found that NRK-52E cells exposed to HG exhibited a loss of mitochondrial membrane potential, depletion of ATP, enhanced cytochrome c release and increased caspase-9 and -3 activation, and ultimate cellular breakdown. Our data showed that erianin protected NRK-52E cells against HG-induced damage by ameliorating all of these events, resulting in reduced apoptosis and increased viability. The data suggest that erianin alleviates HG-induced cytotoxicity in NRK-52E cells, at least in part, by reversing the mitochondrial cytochrome c-activated caspases signaling pathway.

Hyperglycemia induces the overexpression of p53 and its phosphorylation on Ser15 (activated). This activation of p53 is linked to the downregulation of Bcl-2 and the upregulation of Bax, thus activating the intrinsic apoptotic pathway (42). Consistent with these findings, we also found that exposure to HG induced the phosphorylation of p53 on Ser15 and increased p53 expression in NRK-52E cells. Treatment with erianin abrogated the expression and phosphorylation of p53 induced by the exposure to HG. Therefore, the present study also evaluated the link between erianin exposure and HG-induced mitochondrial dysfunction by studying Bax and Bcl-2. As a result, due to the fact that erianin blocks HG-induced elevation of Bax and decreases Bcl-2 in HG exposed NRK-52E cells, it normalizing the ratio of Bax/Bcl-2. Thus, erianin protects NRK-52E cells against HG-induced mitochondria-mediated apoptosis partly by restoring the balance of anti-apoptotic and pro-apoptotic proteins which could be considerable.

HG increased renal tubular cells apoptosis through the enhanced generation of ROS as well as changes in the MAPK-dependent signal transduction pathways has been documented (Wang et al., 2017). In hyperglycaemic status, ROS also leads to activation of some transcription factors such as NF-kB, which eventually lead to a change in expression patterns of genes that are essential for the induction of apoptosis (Sanchez and Sharma, 2009). It seems that MAPK/NF-κB activation is involved in the pathogenesis of HG-induced cell dysfunction and apoptosis, suggesting that agents which can block MAPK/NF-κB signaling might be effective in treating diabetes complications (Sakai et al., 2005). Regulating the activity of the MAPK signaling pathway, particularly the activation of JNK and p38, is vital for protecting cells from ROS injury and cellular death (Peti and Page, 2013). Therefore,

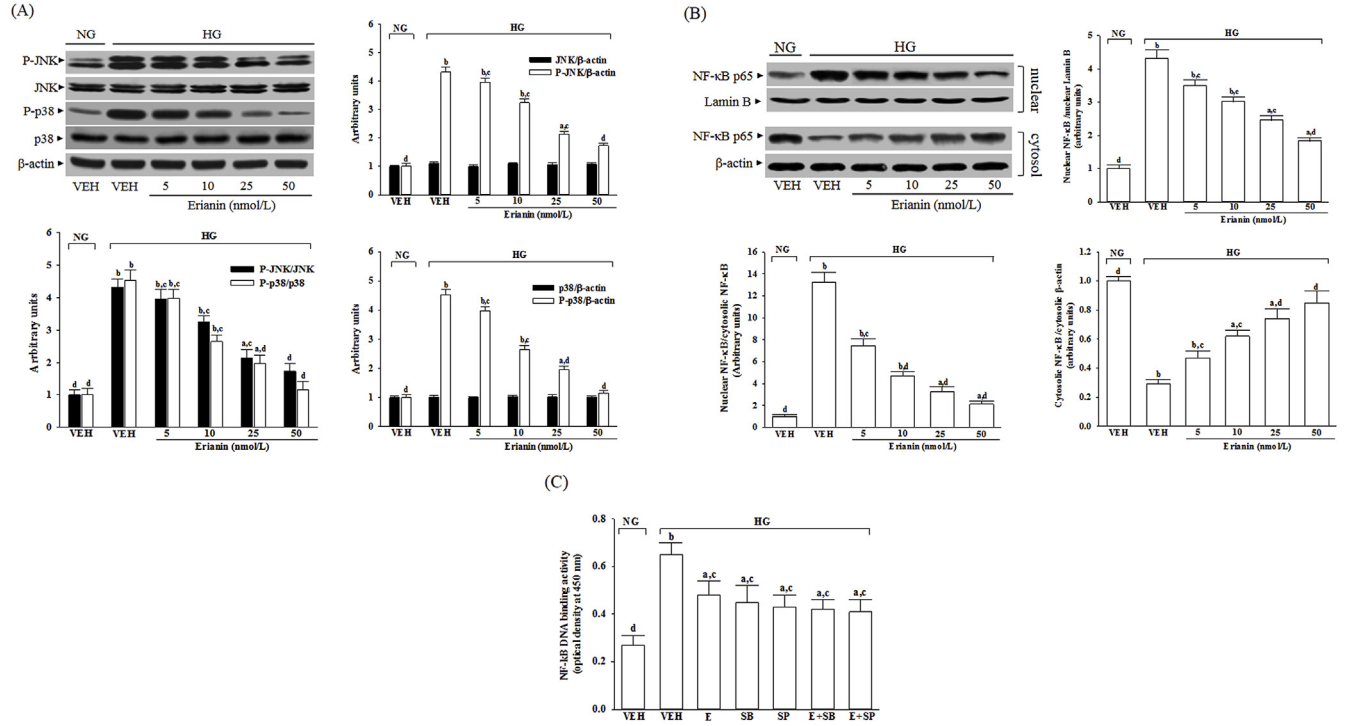

Fig. 5. Effect of erianin on activation of JNK, p38 and NF-κB in high glucose cultured NRK-52E cells. Cells were pretreated with different concentrations of erianin (5, 10, 25 or 50 nmol/L) for 1 h and then exposed to exposure to normal (NG), or high (HG) glucose for an additional 48 h. (A) The photographs were representatives the Western blots for p-JNK, JNK, p-p38 and p38. The ratios of p-p38/p38 and p-JNK/JNK were calculated. (B) The densities of protein bands for NF-κB p65 in nuclear and cytosolic fractions of cells were quantitated and the nuclear-to-cytosolic protein expression ratio of NF-κB p65 was calculated. (C) DNA-binding activity of NF-kB p65 in the nuclear extracts of NRK-52E cells after indicated treatments as measured by an ELISA-based TransAM® kit. In this assay, the NRK-52E cells were pretreated with the SB203580 (SB), or SP600125 (SP) at 10 μmol/L for 30 min and then incubated with erianin (E; 50 nmol/L) or vehicle (VEH) for 1 h followed by exposure to NG or HG medium for 48 h. The experiments were performed in triplicate and data are presented as the mean ± S.D. of five independent experiments (n = 5). $^{a}p < 0.05$ and $^{b}p < 0.01$ when compared to the vehicle-treated control group cultured in NG medium. $^{c}p < 0.05$ and $^{d}p < 0.01$ when compared to the VEH-treated group cultured in HG medium.

we investigated whether the protective effect of erianin against HG-induced renal damage and dysfunction involves its ability to repress inhibiting the ROS-mediated JNK, p38, and NF-κB pathways. To further confirm whether JNK and p38 activation contributed to ROS-triggered apoptosis in NRK-52E cells, SP600125 (a pharmacological inhibitor of JNK) and SB203580 (a pharmacological inhibitor of p38) were used. Both SB203580 and SP600125 suppressed the DNA-binding activity of NF-kB p65 in NRK-52E cells incubated in culture medium containing high levels of glucose, suggesting activation of JNK and p38 are required and involved in HG-induced NF-κB activation. Similarily, erianin protected the NRK-52E cells from HG-induced cytotoxicity and apoptosis, and resulted in a parallel decrease in the phosphorylation degree of JNK and p38, finally remarkable down regulated the NF-kB DNA-binding activity in NRK-52E cells exposured to HG. In addition, neither SP600125 nor SB203580 blocked the inhibitory effect of erianin in the HG cultured NRK-52E cells. The results suggested that the renal protective properties of erianin were associated with suppressing ROS mediated JNK/p38-MAPK and NF-κB signaling, consequently affecting the expression of apoptosis associated genes. Thus, our findings support a protective role of erianin in NRK-52E cells exposed to a HG challenge through the suppression of the ROS/MAPK/NF-κB signaling pathways.

5. Conclusions

In conclusion, our study demonstrates that sustained HG-stimulated NRK-52E cell apoptosis, and erianin alleviates renal tubular epithelial cell apoptosis in HG condition may by reducing oxidative stress through suppression of MAPK and NF-κB activation. These findings would possibly open a new venue for erianin as a therapeutic strategy in renal tubular injury induced by hyperglycemia.

Conflicts of interest

The authors declare no conflicts of interest in relation to this work.

Funding

The present study was partly supported by a grant from the Ministry of Science and Technology (MOST 107-2320-B-127-001) of Taiwan.

Appendix A. Supplementary data

Supplementary data to this article can be found online at https://doi.org/10.1016/j.fct.2019.02.021.

References

Chinese Pharmacopeia Commission, 2010. Pharmacopoeia of the People's Republic of China, vol. 1. China Medical Science Press, Beijing, pp. 150–151.
Czajka, A., Malik, A.N., 2016. Hyperglycemia induced damage to mitochondrial respiration in renal mesangial and tubular cells: implications for diabetic nephropathy. Redox. Biol. 10, 100–107.
Esterbauer, H., Cheeseman, K.H., 1990. Determination of aldehydic lipid peroxidation products: malonaldehyde and 4-hydroxynonenal. Methods Enzymol. 1990, 407–421.
Gerlier, D., Thomasset, T., 1986. Use of MTT colorimetric assay to measure cell activation. J. Immunol. Methods 94, 57–63.
Gong, C.Y., Yu, Z.Y., Lu, B., Yang, L., Sheng, Y.C., Fan, Y.M., Ji, L.L., Wang, Z.T., 2014. Ethanol extract of Dendrobium chrysotoxum Lindl ameliorates diabetic retinopathy and its mechanism. Vasc. Pharmacol. 62, 134–142.
Hu, J., Fan, W., Dong, F., Miao, Z., Zhou, J., 2012. Chemical components of dendrobium chrysotoxum. Chin. J. Chem. 30, 1327–1330.
Hüttemann, M., Helling, S., Sanderson, T.H., Sinkler, C., Samavati, L., Mahapatra, G., Varughese, A., Lu, G., Liu, J., Ramzan, R., Vogt, S., Grossman, L.I., Doan, J.W., Marcus, K., Lee, I., 2012. Regulation of mitochondrial respiration and apoptosis through cell signaling: cytochrome c oxidase and cytochrome c in ischemia/

reperfusion injury and inflammation. Biochim. Biophys. Acta 1817, 598–609.
Kaja, S., Payne, A.J., Naumchuk, Y., Koulen, P., 2017. Quantification of lactate dehydrogenase for cell viability testing using cell lines and primary cultured astrocytes. Curr. Protoc. Toxicol. 72, 2.26.1–2.26.
Kimmich, G.A., Randles, J., Brand, J.S., 1975. Assay of picomole amounts of ATP, ADP, and AMP using the luciferase enzyme system. Anal. Biochem. 69, 187–206.
Kreider, K.E., Gabrielski, A.A., Hammonds, F.B., 2018. Hyperglycemia syndromes. Nurs. Clin. North. Am. 53, 303–317.
Lam, Y., Ng, T.B., Yao, R.M., Shi, J., Xu, K., Sze, S.C., Zhang, K.Y., 2015. Evaluation of chemical constituents and important mechanism of pharmacological biology in dendrobium plants. Evid. Based Complement. Alternat. Med. 841752.
Lowry, O.H., Rosebrough, N.J., Farr, A.L., Randall, R.J., 1951. Protein measurement with the Folin phenol reagent. J. Biol. Chem. 193, 265–275.
Luna-Vargas, M.P., Chipuk, J.E., 2016. The deadly landscape of pro-apoptotic BCL-2 proteins in the outer mitochondrial membrane. FEBS J. 283, 2676–2689.
Lv, S.Q., Zhang, S.F., Su, X.H., 2018. Experience in treating diabetic nephropathy by strengthening spleen and strengthening kidney, removing blood stasis and dredging collaterals. Guiding J. Tradit. Chin. Med. Pharm. 24, 121–123.
Ma, G.X., Xu, G.J., Xu, L.S., 1994. Inhibitory effects of Dendrobium chrysotoxum and its constituents on the mouse HePA and ESC. J. China Pharm. Univ. 25, 188–189.
Németh, I., Boda, D., 1989. The ratio of oxidized/reduced glutathione as an index of oxidative stress in various experimental models of shock syndrome. Biomed. Biochim. Acta 48, 53–57.
Ng, T.B., Liu, F., Wang, Z.T., 2000. Antioxidative activity of natural products from plants. Life Sci. 66, 709–723.
Owen, J.B., Butterfield, D.A., 2010. Measurement of oxidized/reduced glutathione ratio. Methods Mol. Biol. 648, 269–277.
Pérez, M.J., Quintanilla, R.A., 2017. Development or disease: duality of the mitochondrial permeability transition pore. Dev. Biol. 426, 1–7.
Peti, W., Page, R., 2013. Molecular basis of MAP kinase regulation. Protein Sci. 22, 1698–1710.
Pugliese, G., 2014. Updating the natural history of diabetic nephropathy. Acta Diabetol. 51, 905–915.
Rani, V., Deep, G., Singh, R.K., Palle, K., Yadav, U.C., 2016. Oxidative stress and metabolic disorders: pathogenesis and therapeutic strategies. Life Sci. 148, 183–193.
Rastogi, R.P., Singh, S.P., Häder, D.P., Sinha, R.P., 2010. Detection of reactive oxygen species (ROS) by the oxidant-sensing probe 2′, 7′-dichlorodihydrofluorescein diacetate in the cyanobacterium Anabaena variabilis PCC 793. Biochem. Biophys. Res. Commun. 397, 603–607.
Sakai, N., Wada, T., Furuichi, K., Iwata, Y., Yoshimoto, K., Kitagawa, K., Kokubo, S., Kobayashi, M., Hara, A., Yamahana, J., Okumura, T., Takasawa, K., Takeda, S., Yoshimura, M., Kida, H., Yokoyama, H., 2005. Involvement of extracellular signal-regulated kinase and p38 in human diabetic nephropathy. Am. J. Kidney Dis. 45, 54–65.
Sanchez, A.P., Sharma, K., 2009. Transcription factors in the pathogenesis of diabetic nephropathy. Expert Rev. Mol. Med. 11, e13.
Sifuentes-Franco, S., Padilla-Tejeda, D.E., Carrillo-Ibarra, S., Miranda-Díaz, A.G., 2018. Oxidative stress, apoptosis, and mitochondrial function in diabetic nephropathy. Internet J. Endocrinol. 1875870 2018.
Sinha, K., Das, J., Pal, P.B., Sil, P.C., 2013. Oxidative stress: the mitochondria-dependent and mitochondria-independent pathways of apoptosis. Arch. Toxicol. 87, 1157–1158.
Slyne, J., Slattery, C., McMorrow, T., Ryan, M.P., 2015. New developments concerning the proximal tubule in diabetic nephropathy: in vitro models and mechanisms. Nephrol. Dial. Transplant. 30 (Suppl. 4), iv60–i67.
Tsikas, D., 2017. Assessment of lipid peroxidation by measuring malondialdehyde (MDA) and relatives in biological samples: analytical and biological challenges. Anal. Biochem. 524, 13–30.
Vakifahmetoglu-Norberg, H., Ouchida, A.T., Norberg, E., 2017. The role of mitochondria in metabolism and cell death. Biochem. Biophys. Res. Commun. 482, 426–431.
Vallon, V., Thomson, S.C., 2012. Renal function in diabetic disease models: the tubular system in the pathophysiology of the diabetic kidney. Annu. Rev. Physiol. 74, 351–375.
Volpe, C.M.O., Villar-Delfino, P.H., Dos Anjos, P.M.F., Nogueira-Machado, J.A., 2018. Cellular death, reactive oxygen species (ROS) and diabetic complications. Cell Death Dis. 9, 119.
Wang, Y., Zhang, J., Zhang, L., Gao, P., Wu, X., 2017. Adiponectin attenuates high glucose-induced apoptosis through the AMPK/p38 MAPK signaling pathway in NRK-52E cells. PLoS One 12, e0178215.
Yang, S., Han, Y., Liu, J., Song, P., Xu, X., Zhao, L., Hu, C., Xiao, L., Liu, F., Zhang, H., Sun, L., 2017. Mitochondria: a novel therapeutic target in diabetic nephropathy. Curr. Med. Chem. 24, 3185–3202.
Yu, Z., Gong, C., Lu, B., Yang, L., Sheng, Y., Ji, L., Wang, Z., 2015. Dendrobium chrysotoxum Lindl. Alleviates diabetic retinopathy by preventing retinal inflammation and tight junction protein decrease. J. Diabetes Res. 2015, 518317.
Yu, Z., Zhang, T., Gong, C., Sheng, Y., Lu, B., Zhou, L., Ji, L., Wang, Z., 2016. Erianin inhibits high glucose-induced retinal angiogenesis via blocking ERK1/2-regulated HIF-1α-VEGF/VEGFR2 signaling pathway. Sci. Rep. 28, 6.
Zhang, X., Zhao, Y., Chu, Q., Wang, Z.Y., Li, H., Chi, Z.H., 2014. Zinc modulates high glucose-induced apoptosis by suppressing oxidative stress in renal tubular epithelial cells. Biol. Trace Elem. Res. 158, 259–267.
Zhao, L., Zhang, H., Bao, J., Liu, J., Ji, Z., 2015. Saikosaponin-d protects renal tubular epithelial cell against high glucose induced injury through modulation of SIRT3. Int. J. Clin. Exp. Med. 8, 6472–6481.